Low Velocity Impact Properties of 3D Auxetic Textile Composite

Lin ZHOU, Jifang ZENG, Lili JIANG, Hong HU*

Institute of Textiles and Clothing, The Hong Kong Polytechnic University, Hung Hom, Kowloon, Hong Kong

*Corresponding author: Tel: +852-3400 3089 Email Address: hu.hong@polyu.edu.hk

Abstract

3D auxetic textile composites are a special type of auxetic materials which have attracted more attention in recent years. Their deformation behaviour and mechanical properties under quasi-static compression have been investigated in the previous studies. In this paper, a further study on their mechanical properties under low velocity impact is presented. Both single and repeating impact tests were conducted at different impact energy levels ranging from 12.7 J to 25.5 J. Results show that the 3D auxetic textile composite has better impact protective performance than the 3D non-auxetic textile composite due to better transmitted force reduction and higher energy absorption capacity under single-time impact and higher structural stability under repeating impacts. The results also show that the difference in protective performance between the auxetic and non-auxetic textile composites get increased with the increase of impact energy.

Keywords: 3D auxetic composites; negative Poisson's ratio (NPR); low velocity impact; energy absorption; textile composites

1. Introduction

Auxetic composites are an important category of auxetic materials, which have been proven to have a number of enhanced properties compared with non-auxetic composites, such as enhanced impact resistance [1, 2], increased energy absorption ability[3, 4] and improved mechanical indentation resistance [5]. These properties have led to many interesting applications including protective equipment [6]. Up to date, there are mainly two approaches for fabricating auxetic composites. The first one is utilizing conventional components like off-the-shelf prepregs via specially designed configurations to achieve auxetic behavior in a laminated composite [7-9]. Another approach is employing intrinsically auxetic components including auxetic structures or networks [10], auxetic fabrics [11], and auxetic fibres [12] into a conventional matrix material to form so called network-embedded composites [13]. In 1992, Milton [14] firstly proposed the possibility of producing composite laminates with a predicted Poisson's ratio closed to -1.

The experimental studies of the impact properties of auxetic composite materials can be generally divided into high velocity and low velocity impact tests [15]. One of the important type of low velocity impact tester is drop weight tester that could measure the impact performance of an entire structure under out-of-plane impact loads. Moreover, the drop weight tester can be adapted to different testing conditions including the shape of impactor, boundary conditions and impact energy.

The low velocity impact properties of auxetic polymers especially auxetic foams have been investigated by various researchers [16-18]. Scarpa et al. experimentally evaluated the auxetic polyurethane (PU) foams under impact drop tests with a velocity of 1.5m/s and compared these auxetic foams with conventional foams [17]. The Poisson's ratio of the auxetic foams they used for test was -0.04. Their tests showed that the open-cell auxetic foam greatly increased the crashworthiness qualities of the open-cell foam. They also found that the auxetic foam showed structural integrity feature under dynamic loading and suggested to use auxetic foam to enhance the energy absorption capacity of self-sensing structural components due to large displacement given by auxetic effect [17]. Lisiecki et al. [19] manufactured auxetic foams via a novel Mechanic-Chemic-Thermal (M-Ch-T) manufacturing process. The highest negative Poisson's ratio of produced samples could reach -0.125. The researchers also investigated deformation behaviour and mechanical properties under compression and dynamic drop tests. Auxetic foams exhibited higher energy density values and lower values of deceleration thus they could be applied as cushioning material. Allen et al. [20] reported the quasi-static and low-kinetic energy impact behaviour of conventional and auxetic open-cell foams that were manufactured by thermos-mechanical process. Auxetic foams that showed a six times reduction in peak acceleration compared to their conventional counterpart have exhibited potential for protective applications.

However, few investigations have been carried out on the impact properties of fibre reinforced auxetic composites. In previous studies of fibre reinforced composite materials under low velocity impact test, Zhou et al. [21] experimentally and numerically studied impact energy absorption properties of the composites reinforced by the multiaxial warp knitted structure. Alderson et al. manufactured auxetic carbon fibre laminates by using off-the-shelf prepreg material and the conventional vacuum bag moulding technique [1] and evaluated their low velocity impact resistance in comparison with two laminates having near zero(+0.086) and large Poisson's ratio (+0.187) [22]. They also compared the impact test results with those obtained from static compression tests. The results showed that the impact performance of auxetic laminates had increasing loads to the first failure (occurred at around 7J) with enhanced energy absorption. Compared with the performance under low velocity impact, the laminates under static compression tests exhibited higher loads and absorbed more energy to catastrophic failure. Recently, Liaqat et al. [23] proposed a novel 3D auxetic woven structure based a modified four-layer woven structure through the thickness. The 3D woven fabrics were transformed into composites by vacuum-assisted resin transfer moulding. The highest achieved negative Poisson's ratio of the composite was -2.08. Their study showed that energy absorption ability of 3D auxetic woven composites was 6.7% higher than that of non-auxetic composites.

By eliminating the stitch yarns in a 3D auxetic textile structure which had been proposed by Ge et al. [10, 24, 25], Jiang et al. recently proposed a new process of

fabricating auxetic composites by using multilayer orthogonal auxetic structure as reinforcement and PU foam as matrix [26]. More recently, they evaluated the energy absorption and impact resistance of these auxetic composites and compared them with polymeric foams and non-auxetic composites [27]. Their study indicated that the auxetic and non-auxetic composites have different mechanical responses under impact energies ranging from 7.25J to 65.25J due to different deformation mechanisms. Their study also showed that auxetic composites had enhanced energy absorption performance in medium strain range. Recently, Zhou et al. conducted an experimental study on the deformation behaviours and mechanical properties of the 3D auxetic textile composite under quasi-static compression and compared with those of the pure PU foam and non-auxetic textile composite made with the same materials and structural parameters but with different yarn arrangement [28]. Meanwhile, Zeng et al. also conducted a finite element (FE) analysis on the same type of auxetic textile composite [29]. Both experimental and FE analysis confirmed excellent auxetic behaviour of 3D auxetic textile composites under quasi-static compression. However, there is a lack of investigation on the deformation behaviour of auxetic textile composites under impact conditions. Therefore, a further study on 3D auxetic textile composites under low velocity impact was conducted and presented in this paper. It is expected that this study could help us to better understand the impact properties of these auxetic textile composites in order to promote their application for impact protection.

2. Experimental details

2.1 Preparation of 3D textile composites

The 3D auxetic composite was fabricated by using 3D auxetic textile structure as reinforcement and conventional PU foam as matrix. As shown in Fig. 1a, the 3D auxetic textile structure consists of three yarns systems: weft yarn, warp yarn and stitch yarn. The rigid polyamide filaments are stacked layer by layer as weft yarns and the braided cotton yarns are stacked in staggered form layer by layer as warp yarns. Both the warp and weft yarns are bound together with polyester multifilament to form an integrated 3D textile structure. For comparison, the non-auxetic composite was also fabricated using the same yarns and PU foam by arranging the warp yarns in a different way, as shown in Fig.1b. Different from the auxetic composite, the warp yarns in non-auxetic composite are stacked in non-staggered type. The details of the 3D textile reinforcement structures are listed in Table 1. A customized mould made of stainless steel for fabrication of 3D auxetic textile structure was used to fabricate the 3D textile reinforced structures, as illustrated in Fig. 2a.

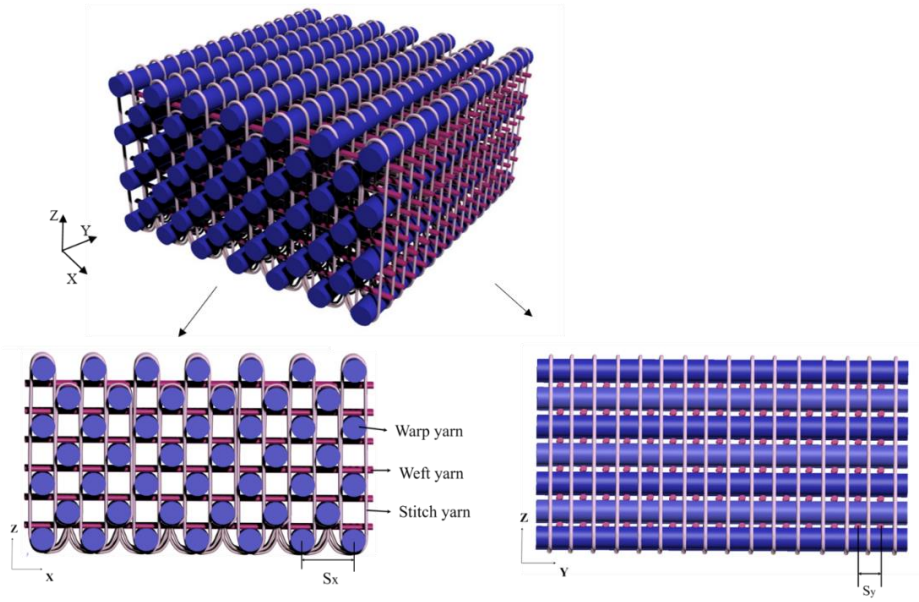

(a)

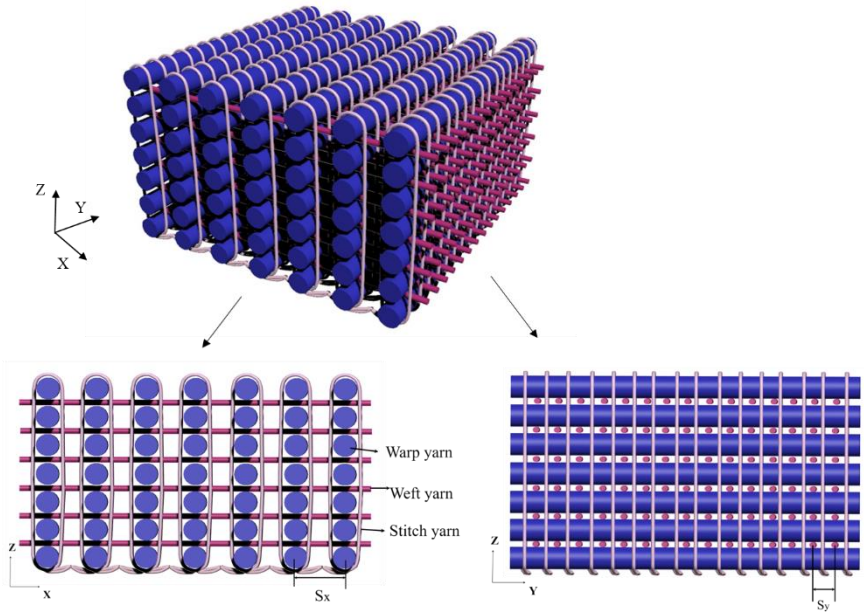

(b)

Fig. 1 3D textile structures: (a) auxetic; (b) non-auxetic.

Table 1 Details of 3D auxetic and non-auxetic textile structures produced

Structure name	Warp yarn		Weft yarn		Diameter of stitch yarn (mm)	Fabric structure thickness (mm)
	Diameter (mm)	Spacing S_x (mm)	Diameter (mm)	Spacing S_y (mm)		
Auxetic composite	4	15	2	7.5	0.5	46
Non-auxetic composite	4	15	2	7.5	0.5	47

With the use of these 3D textile structures, both the auxetic and non-auxetic composites were fabricated through an injection and foaming fabrication process. To facilitate the manufacturing process of 3D auxetic textile composites, a customized mould made of Polytetrafluoroethene (PTFE) is adopted, as show in Fig. 2b. The fabrication process is schematically shown in Fig. 3 and its details can be found in [28]. The matrix used was formed with the chemical solution (Cst-1087A/B PU foam) which was uniformly mixed with PU resin composition (polyether polyol, catalysts and blowing agents) and MDI (isocyanate). All chemical solutions were in analytical grade and used directly without further purification. The 3D auxetic and non-auxetic composites fabricated are shown in Fig. 4. The dimensions of samples produced used for tests were approximately 10cm × 10cm × 6cm. The pure PU foam block made of the same dimensions was also made for the comparison purpose.

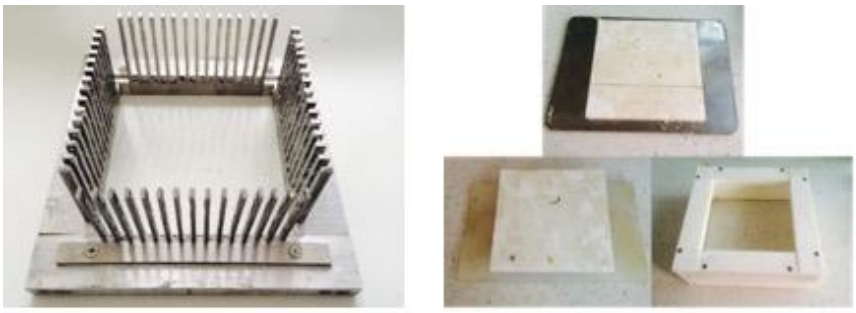

(a) (b)

Fig.2 The customized (a) stainless steel mould and (b) PTFE moulds for fabricating 3D textile structures and composites

(a) (b) (c) (d)

Fig. 3 Schematic presentation of fabrication process for 3D textile composites

(a) (b)

Fig. 4 3D textile composites fabricated: (a) auxetic; (b) non-auxetic.

2.2 Impact and quasi-static compression tests

The low velocity impact tests were conducted on a drop-weight impact tester KD-3168-E manufactured by King Design Company in Taiwan. As shown in Fig. 5, the impact tester used a drop striker with a 150mm circular flat surface at impact side. The total weight of the striker was 6.5kg. The drop striker was instrumented with an ISOTRON accelerometer (with a sensitivity of 9.929mV/g and a measuring range of ±500g) to measure the acceleration. The transmitted force was measured by a load cell (1210AF-50KN from Interface Inc. Scottsdale, Arizona, USA, with a sensitivity of 4.171mV/g) installed on a massive base with a weight of 1000kg. During impact test, the sample was stuck on the anvil installed on the base. All the measurement signals were recorded by a high-speed data acquisition card NI6040E having a recording frequency of 80kHz.

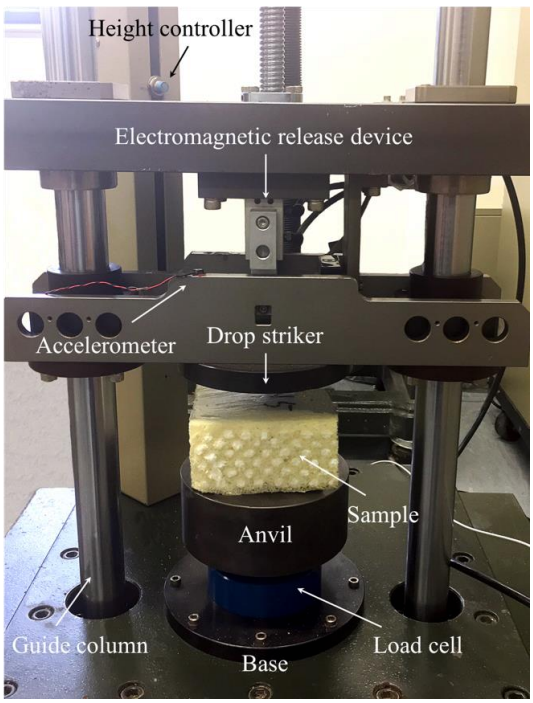

Fig. 5 Drop-weight impact tester.

The impact test was performed according to ASTM D 1596-97 (Standard Test Method for Dynamic Shock Cushioning Characteristics of Packaging Material), based on the drop-weight principle using a low-energy and a low-speed impact tester that can measure the changes in acceleration of the drop striker and the force transmitted from the top side to the bottom side of the specimen. The transmitted force is obtained directly from the load cell. But the contact force is proportional to the measured acceleration and can be calculated from Newton's second law. Because it is freely falling, the maximum velocity of the striker is determined by the drop height when the striker just falls onto the top surface of the sample. Using the maximum velocity of the striker as the initial value, the velocity of the striker can be calculated by integrating the acceleration of the striker after it has contacted the sample. Meanwhile, the impact displacement can be obtained by integrating this velocity of the striker, assuming the time is zero when the initial contact occurs. Due to the slightly difference in the thickness of each specimen, the impact strain was used for analysis and comparison instead of displacement. Before impact test, all the test specimens were preprocessed in an environment of 20℃ and 65% relative humidity. The auxetic and non-auxetic composites were tested with varied impact energy levels (from 12.7J to 31.9J) to make a comparison on their impact protection properties. Based on the impact force and displacement obtained from the impact test, the energy absorption (E_a) of each composite was calculated from equation $a = \int_0^s F(x)ds$, where s is the impact displacement and F is the impact force. In order to investigate the structural stability under continuous impact, the repeating impact tests were also conducted for both the

auxetic and non-auxetic textile composites at two impact energy levels (19.1J and 31.9J). Due to the time required for the striker to go back to its initial impact height, the time interval between two impacts was 30s in this work.

In addition to the impact test, the quasi-static compression test was also conducted on an Instron 5566 Universal Testing Machine at a speed of 0.5mm/s up to 55% deformation strain to measure the Poisson's ratio of both the auxetic and non-auxetic textile composites and assist to investigate their impact protection ability. The load cell capacity of the testing device is 10kN. The detail quasi-static compression test conditions can be found in our previous paper [28]. To measure the transversal and vertical size change of the produced composites, as illustrated in Fig. 6, four black points were marked on the cross-section of each specimen to facilitate recording the deformation during testing process. A camera Canon PowerShot G10 with a timer shot function was placed at a distance of 50cm from the tested specimen to take photos of the marked points. As shown in Fig. 6, H is the distance between the two marked points in the vertical direction and L is the distance between the two marked points in the horizontal direction. H_0 and L_0 are their initial values. A screen ruler was used to measure the distances of the black marked points from the photos during the compression process. According to the measured results, the compression strain ε_z and transversal strain ε_x could be calculated from Eq. (1) and (2).

$$\varepsilon_z = \frac{H - H_0}{H_0} \quad (1)$$

$$\varepsilon_x = \frac{L - L_0}{L_0} \quad (2)$$

Finally, Poisson's ratio ν could be calculated from Eq. (3).

$$v = -\frac{\varepsilon_x}{\varepsilon_z} \quad (3)$$

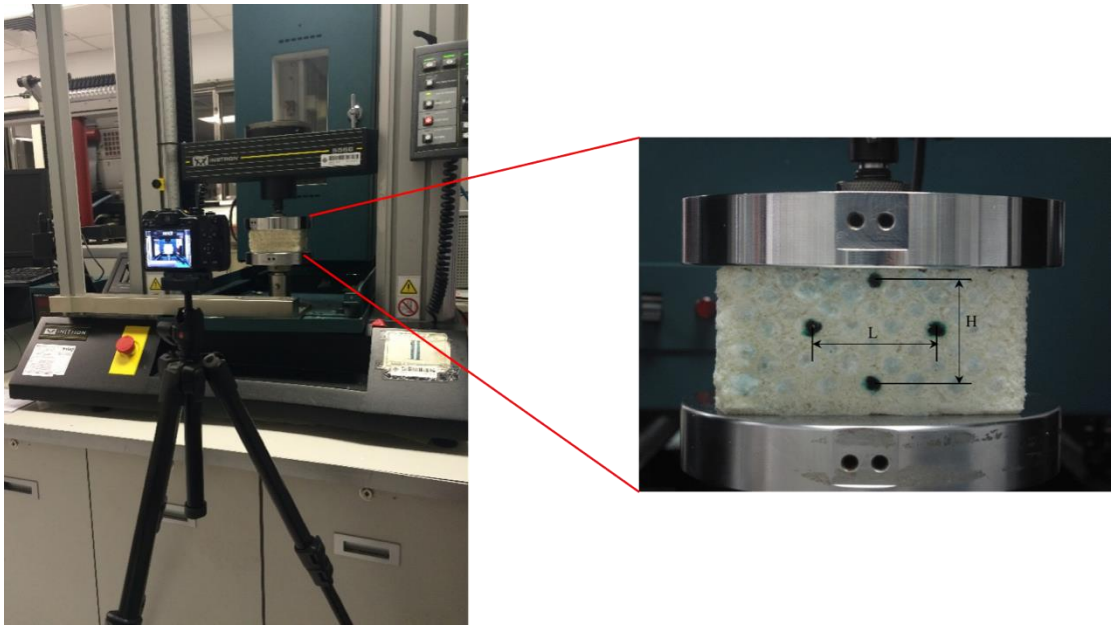

Fig. 6 Set-up of the testing system.

3. Results and discussion

3.1 Deformation behaviour under quasi-static compression

Before discussing the impact properties of auxetic and non-auxetic textile composites, it is necessary to understand their deformation behaviour and mechanical properties under quasi-static compression. As shown in Fig. 7, the pure PU foam, the auxetic and non-auxetic textile composites presents different Poisson's ratio variation trends under

quasi-static compression. For the PU foam, the quasi-zero Poisson's ratio appears at the initial stage of compression process. This quasi-zero Poisson's ratio phenomenon is mainly caused by porous structure of the foam. During the initial stage of compression, the pores in the inner foam was compressed solely along the loading direction, while the transverse dimension of pores is still kept almost constant. However, with the increase of compression strain, the Poisson's ratio of the foam positively increases and reaches a maximum value of about 0.075 at a compression strain of 18%, and then slowly decreases until the end of the testing at a compression of strain 54.4%. This Poisson's ratio change is due to pores shape changes and crashes within the foam under different compression levels. Under lower compression strains, pores have only shape changes and these changes can lead to a size increase of the foam in the transversal direction. However, with further increase of compression strain, the pores start to crash and the foam is being compacted. As a result, the foam size in the transversal direction starts to decrease, causing a decrease of positive Poisson's ratio value.

For the auxetic and non-auxetic textile composites, the quasi-zero Poisson's ratio also exists because their deformation at the initial stage of compression is mainly determined by the deformation of the pure PU foam due to the specialty of structural arrangement. As shown in Fig. 4, the gaps between layers of inner reinforcements and the peripheries of the reinforcements are filled with PU foam. As the PU foam has much low compression stiffness, it is easier to be deformed than the textile reinforcements. Hence, the initial Poisson's ratio values for auxetic and non-auxetic textile composites are near

zero. However, with the continuity of the compression process, the variation trends in Poisson's ratios of the auxetic and non-auxetic textile composites become totally different. While the Poisson's ratio of the non-auxetic textile composite positively increases with a slower rate, that of the auxetic composite negatively increases with a higher rate. As the auxetic and non-auxetic textile composites were fabricated with the same matrix foam and almost the same volume fraction of reinforcements, the different deformation behaviours of two types of composites mainly arise from different arrangements of warp yarns in the reinforced 3D textile structures, as shown in Fig.1. For the auxetic textile composite, the warp yarns are regularly eliminated in each layer to create void spaces and the weft yarns are arranged in each layer without any elimination. Due to existing of the void spaces, the weft yarns can easily bend under compression of warp yarns when the compression strain increases, which leads to an increased negative Poisson's ratio effect of the composite. The maximum negative Poisson's ratio for the auxetic composite is -0.086 at a compression strain of approximate 38.9%. For the non-auxetic textile composite, the situation is a little more complicated. As the warp yarns are arranged in a form of vertical lines and the distance between the adjacent warp yarns S_x remains the same, the non-auxetic composite can bear larger compression load than the auxetic composite and the weft yarns can be kept in a straight state under compression. In this case, the change of the cross-section of warp yarns from circular to elliptic form under compression can increase the size of the composite in the transversal direction. According to our previous study [28], the warp yarns in the non-auxetic textile composite can keep a stable state until the compression

strain reaches 42.39%. However, as the compression process continues, the warp yarns in the vertical arrangement tend to lose their stability by shifting toward the left or right side of the composite, causing a further increase of the non-auxetic composite in the transversal direction. Thus, the positive Poisson's ratio effect is achieved after the initial stage of the compression process. The maximum positive Poisson's ratio for the non-auxetic composite is 0.024 at a compressive strain of 44.7%. It should be pointed out that the shearing mode may exist after the compression strain exceeds 40%. Therefore, selecting more suitable non-auxetic textile reinforcement structure to avoid possible shearing should be taken in consideration in the future study.

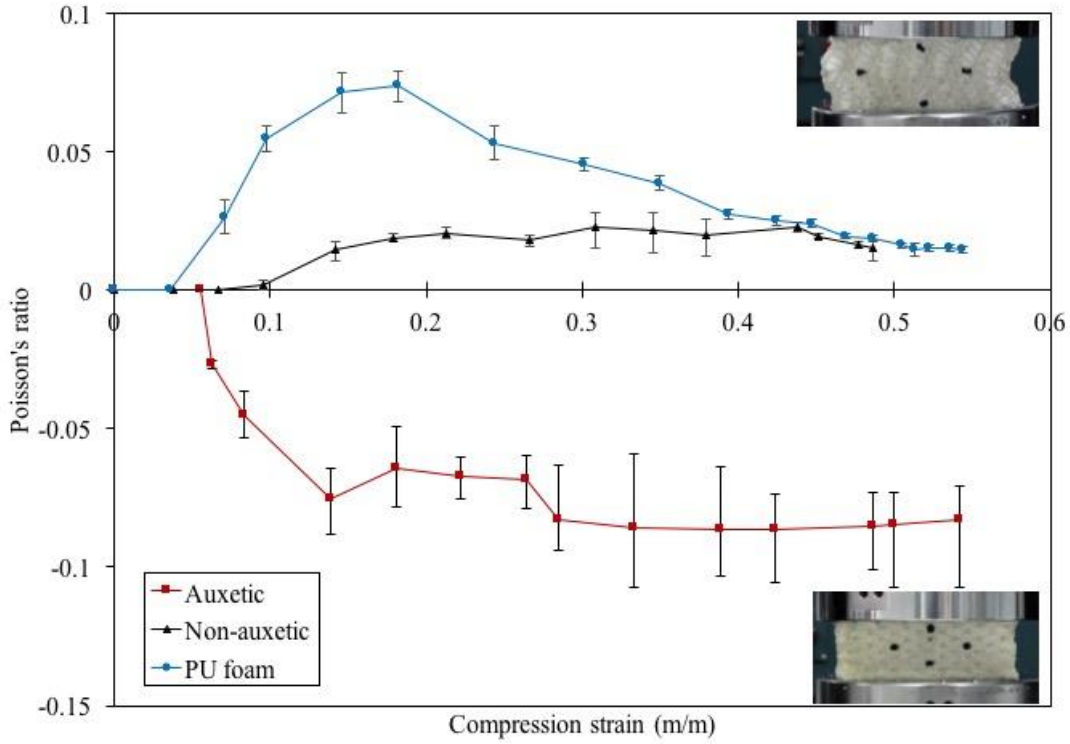

Fig. 7 The Poisson's ratio - strain curves of pure PU foam, 3D auxetic and non-auxetic textile composites. The insert photos show deformation state of auxetic and non-auxetic textile composites under quasi-static compression.

3.2 Treatment of acceleration and transmitted force signals

In this work, Fast Fourier Transform with a low-pass filter was used for filtering the acceleration and transmitted force data of samples under impact tests. Fig. 8 shows the contact acceleration-time and transmitted force-time curves of a tested sample in both original and filtered form at a set cutoff frequency of 400Hz. The cutoff frequency was determined according to MIL-STD-883F Method 2002.4, which indicates that a cutoff frequency of a half-sine waveform should be at least five times of the fundamental frequency of the shock pulse. As shown in Fig. 9, this method also indicates that the pulse duration should be measured between the point at 10% of the peak acceleration during the rising time and the point at 10% of the peak acceleration during the decaying time. Meanwhile, the impact duration should be measured from the beginning to the end of the whole impact process. Taking a non-auxetic composite under 31.9J impact energy as an example, as shown in Fig. 8, the peak acceleration was 487g thus its pulse duration was about 14.2ms. In this case, the cutoff frequency should be higher than 352 Hz. To meet the standard requirement and to obtain a good presentation, 400Hz was used for this sample. Also shown in Fig. 8, the data of the contact acceleration and transmitted force were filtered in such a way that noise was removed but there was sufficient signal remained for the analysis of the curve features. It can be seen that the low-pass filter with this cutoff frequency is effective to eliminate the noise.

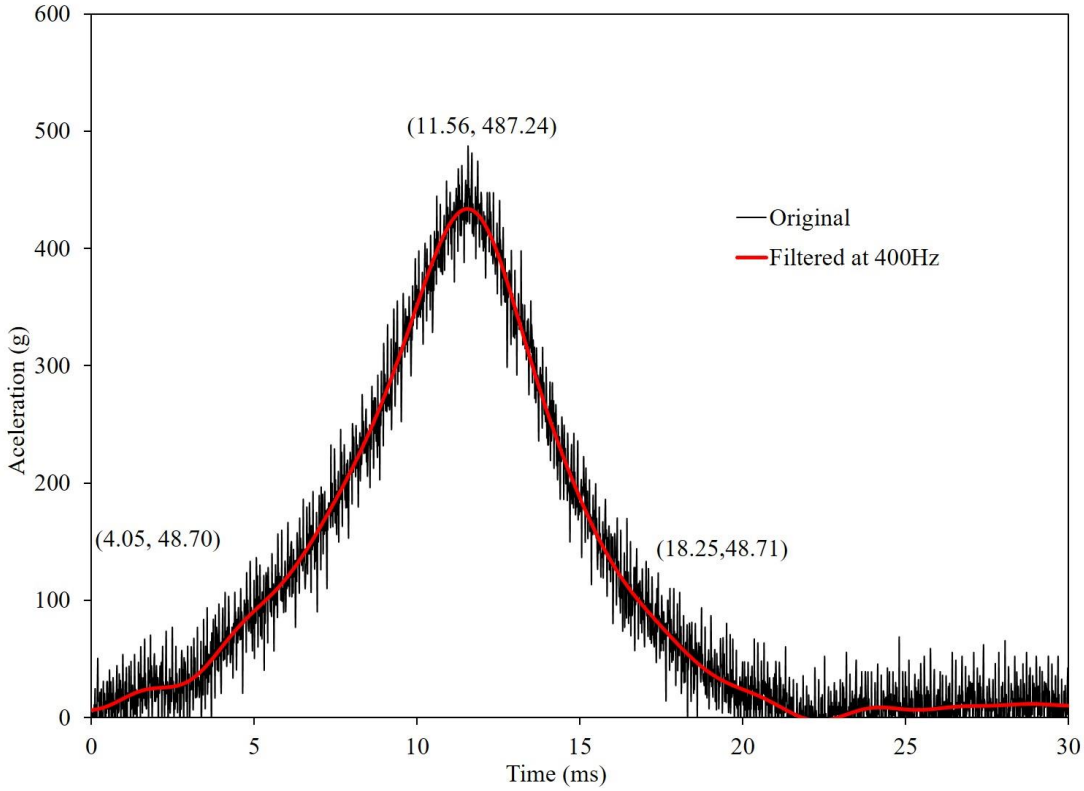
600
500
400
300
200
100
0
Aceleration (g)
(11.56, 487.24)
(4.05, 48.70)
(18.25,48.71)
Original
Filtered at 400Hz
0
5
10
15
20
25
30
Time (ms)

(a)

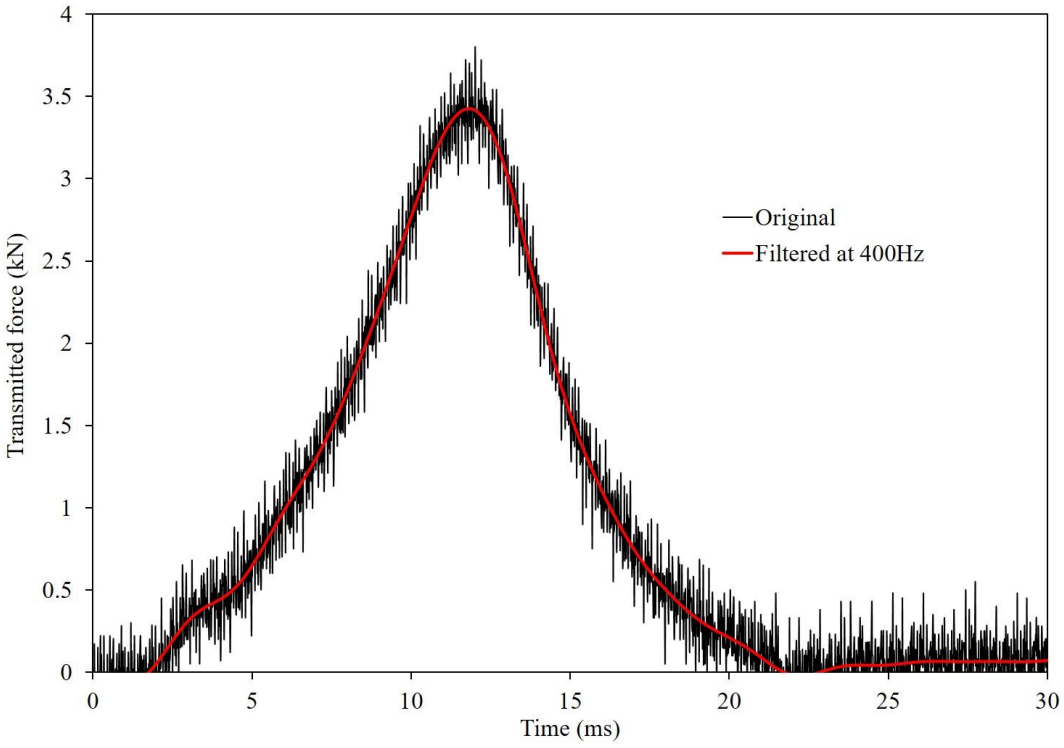
4
3.5
3
2.5
2
1.5
1
0.5
0
Transmitted force (kN)
Original
Filtered at 400Hz
0
5
10
15
20
25
30
Time (ms)

(b)

Fig. 8 Signals in original and after filtering for a non-auxetic composite under 31.9J impact energy: (a) contact acceleration; (b) transmitted force.

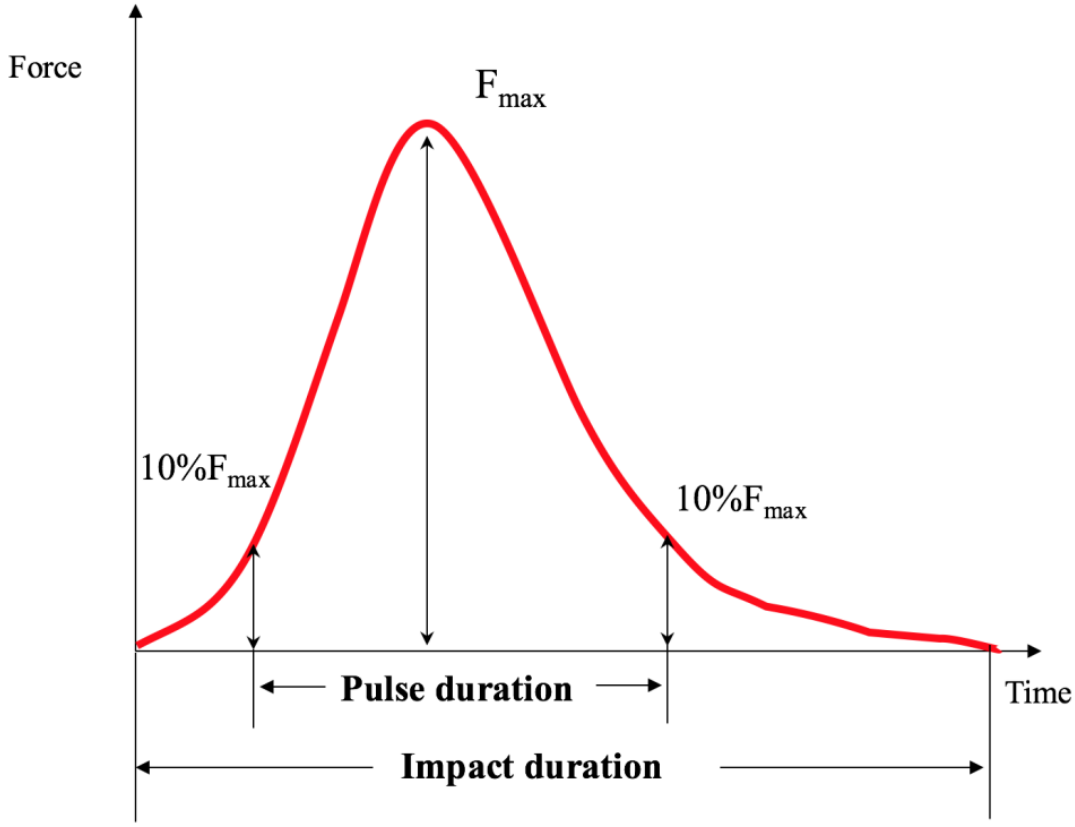

Fig. 9 Schematic demonstration of pulse duration and impact duration

3.3. Impact process analysis

Fig. 10 depicts the representative force-time curves obtained from the low-velocity impact tests for the pure PU foam, the auxetic and non-auxetic textile composites at an impact energy of 19.1J. Among three different materials, the pure PU foam has the highest peak contact and transmitted force, which are 3.62kN and 2.74kN, respectively. Under the same impact energy, the auxetic textile composite has relatively lower peak

contact force and peak transmitted force than those of the non-auxetic textile composite. The peak contact force of the auxetic textile composite is 2.17kN, which is lower than that of the non-auxetic textile composite (2.47kN). And the peak transmitted forces of the auxetic and non-auxetic textile composites are 1.55kN and 1.92kN respectively. Moreover, the impact duration for the PU foam, auxetic and non-auxetic textile composites is 23.3ms, 26.7ms and 25.3ms, respectively. According to the theorem of momentum, a longer impact duration will result in a lower acceleration and a lower dynamic force [30]. The longer impact duration may help to reduce more force and absorb more energy. Thus, among three types of samples, the auxetic textile composite could help to store the impact energy and then release it over a longer time, resulting in a reduction of the contact force and transmitted force. In addition, compared to the contact force curves, the transmitted force curves are relatively smooth and stable. Thus, the auxetic textile composite shows better force reduction than the non-auxetic textile composite under low velocity impact, indicating the auxetic textile composite has better impact protective performance than the non-auxetic textile composite.

From Fig. 10, the force perturbation is also observed in the contact force curve of the auxetic textile composite. It can be seen that there is a sudden force drop (Area A) on the curve, indicating that the weft yarns located at the topside of the auxetic composite are bent by the adjacent warp yarns to cause a force reduction. When the PU foam at the topside is compacted by the bent weft yarns to a certain condition, the impact force begins to increase. As the impact process continues, the force drops occur again in Area

B and Area C, which are also caused by bending of weft yarns in the lower layers. It should be noted that the force drops can result in a reduction of the contact force peak. The contact force drops again after reaching the peak force (2.17kN), and then rebounds. This trend could be attributing to the recovery ability of elastic PU foam as matrix and the load redistribution of the surviving auxetic composite until the impact load has been removed. For the non-auxetic textile composite, its contact force curve has a clear ascending and descending section, which exhibits the stiffening and softening process of the tested specimen. It can be found that there is a plateau (Area D) at the beginning of the impact loading. The main reason is that the PU foam matrix is compressed, but the yarns in the non-auxetic composite have not been compressed at the initial stage of impact. At this stage, the warp yarns are still kept aligned. With the accumulation of impact energy, the warp yarns lose their stability. In this case, the non-auxetic composite is deformed like a buckled bar. As the impact continues, the curve of the non-auxetic composite continues to rise to the peak contact force (2.47kN) without fluctuation. As the warp yarns are arranged in a form of vertical lines in the non-auxetic textile composite, the warp yarns mainly bear the impact load, which lead to higher stiffness and higher contact peak force than the auxetic textile composite under the same impact energy.

Fig. 11 shows the energy versus time curves of the PU foam, auxetic and non-auxetic textile composites when the impact energy is 19.1J. It can be seen that the impact energy absorption of the auxetic textile composite can be divided into three distinct stages. In

the first stage (0~5ms), the value of absorbed energy is relatively low due to small deformation of the foam matrix and insignificant compression of auxetic textile structure. In the second stage (5 -15ms), the energy - time curve increases rapidly and reaches the peak value (19.1J), representing the deformation of the reinforced auxetic textile structure and the increase in vertical displacement of the composite structure. At the last stage (from 15ms to the end), the absorbed energy gradually decreases until the impact process finishes. The whole impact duration of auxetic composite is 26.7ms. Fig. 11 also shows that the absorbed energy of the auxetic composite is 14.3J. For the non-auxetic textile composite, its energy-time curve has similar tendency as that of auxetic textile composite, but the curve of the non-auxetic textile composite reaches its peak value at 13.2ms and then decreases until the impact ends. The energy absorbed by the non-auxetic textile composite is 12.8J. The impact process duration of the non-auxetic textile composite is 25.3ms. For the PU foam, its impact duration is 23.3ms and its curve reaches the peak value at 12.5ms. The energy absorbed by the PU foam is 14.5J. The results show that under the same impact energy, the auxetic textile composite could absorb relatively more energy than the non-auxetic textile composite and PU foam during 15 - 22ms of impact process.

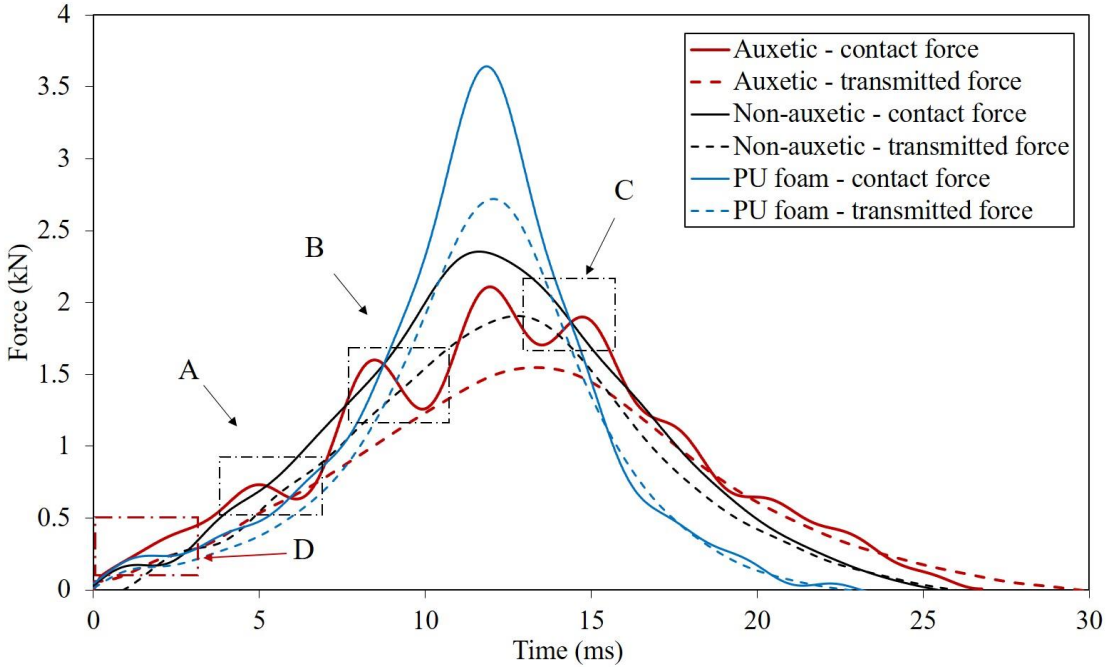

Fig. 10 The contact force and transmitted force curves of PU foam, 3D auxetic and non-auxetic textile composites. Impact energy = 19.1J.

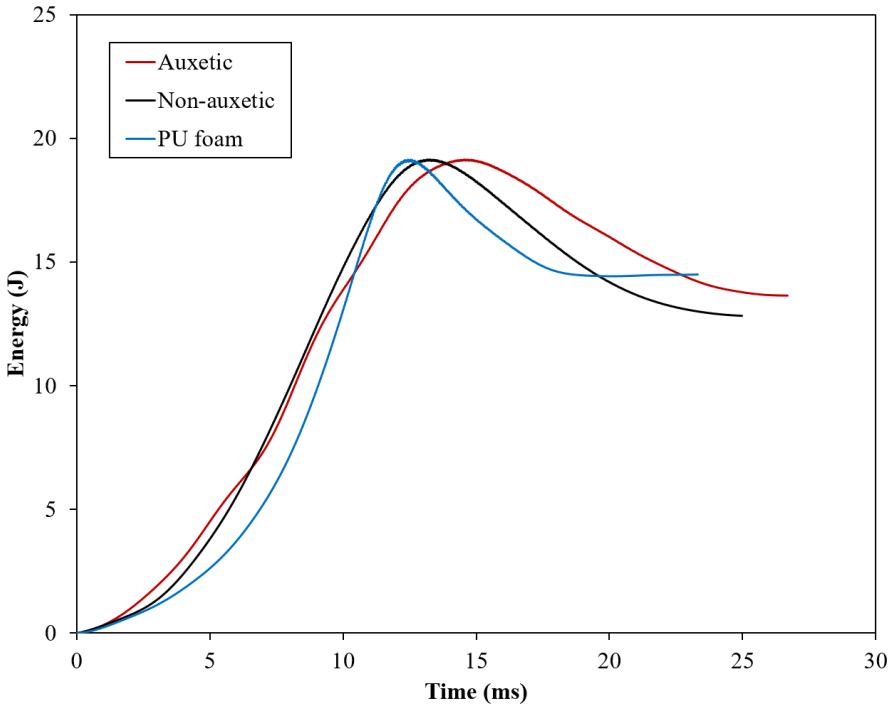

Fig. 11 The energy - time curves of PU foam, 3D auxetic and non-auxetic textile composites. Impact energy = 19.1J

Due to the limitation of the test equipment, it was hard to obtain the Poisson's ratio curve of the auxeti textile composite under flat plate impact tests. Therefore, adopting finite element (FE) method to simulate the Poisson's ratio of the composites under impact could be an alternative. According to our previous FE analysis on the 3D auxetic composite made of multilayer orthogonal reinforcement structure [31], the general variation trends of Poisson's ratio between the quasi-static compression test and the FE impact simulation are the same, but the negative Poisson's ratio value under the quasi-static compression test is higher than that of the FE impact simulation. This difference may come from the hysteresis of impact response. Under the quasi-static compression test, the stress wave is fully propagated among different materials in the composite due to a slow increase rate of compression load (2 mm/min). However, under the impact tests from an impact velocity of 1.50 m/s to 2.67 m/s, the stress wave could not be transmitted to the distant end of the composite in time, therefore, causing the hysteresis of shrinking of the composite in horizontal direction. In other words, the negative Poisson's ratio effect of the auxetic composite from the FE impact simulation is lower

than that from the quasi-static compression. On the other hand, the increase of impact energy could lead to an increase in the maximum negative Poisson's ratio value of the composite since higher impact energy could cause higher compression strain. The FE analysis confirmed that the auxetic composite still retains auxetic characteristic under impact although the auxetic effect is lower than that of the auxetic composite under quasi-static compression.

3.4 Impact compressive behaviour analysis

The contact stress-strain curves and energy absorption-strain curves of the pure PU foam, 3D auxetic and non-auxetic textile composites under the same impact energy (19.1J) are shown in Fig.12 and Fig.13, respectively. For the comparisons, the compression stress-strain curves and energy absorption-strain curves of these materials under quasi-static compression are also presented in these two figures. From Fig. 12, it can be seen that the mechanical behaviors of three types of materials under quasi-static compression are very different. Among three types of materials, the PU foam exhibits a flexible behaviour and has the lowest compression stress. With embedding of textile structures in the PU foam matrix, the compression stress of the textile composites get considerably enhanced. However, due to different arrangement of warp yarns in the textile structure as shown in Fig. 1, two types of textile composites behave differently.

It can be seen that the auxetic textile composite deforms much easier than the non-auxetic textile composite due to easier bending deformation of weft yarns under compression of warp yarns. Therefore, the compression stress of the auxetic textile composite is much lower than that of the non-auxetic textile composite for the same compression strain. For the non-auxetic textile composite, as the warp yarns are arranged in a form of vertical lines, it can bear larger compression load than the auxetic composite under quasi-static compression. However, the difference in mechanical properties among three materials diminishes under the low-velocity impact. As shown in Fig. 12 and Fig. 13, under the low-velocity impact, although the effect of textile reinforcement is still evident as both the contact stress-strain curve and energy-strain curve of the PU foam are much lower than those of two textile composites, the difference between the auxetic and non-auxetic composites become not so evident as the contact stress-strain curves and energy-strain curves of these two composites get closed. Under the quasi-static compression, the energy absorption of the 3D auxetic textile composite is much lower that of the non-auxetic textile composite for the same strain. But under impact, the energy absorption curves of two types of textile composites are almost overlapped, which means that their difference is small. Under impact, the auxetic textile composite even has a little higher energy absorption than the non-auxetic textile composite due to higher deformation. As explained above, the auxetic composite still has negative Poisson's ratio effect under impact, but this effect is considerably reduced if compared with that of the auxetic composite under quasi-static compression. Therefore, the effect of negative Poisson's ratio on the impact

behaviour of the textile composite is reduced, making the auxetic and non-auxetic textile composites have similar responses under impact. However, with the increase of impact energy, the maximum negative Poisson's ratio value of the auxetic composite increases according to the FE simulation. As a result, the effect of negative Poisson's ratio on impact properties will increase too. This phenomenon can be confirmed by Fig. 14, in which the energy absorption of the auxetic textile composite increases faster than that of the non-auxetic textile composite with the increase of impact energy. The results suggest that under lower impact energy, the PU foam plays more important role than textile reinforcement. But with the increase of impact energy, the role of textile reinforcement becomes more important.

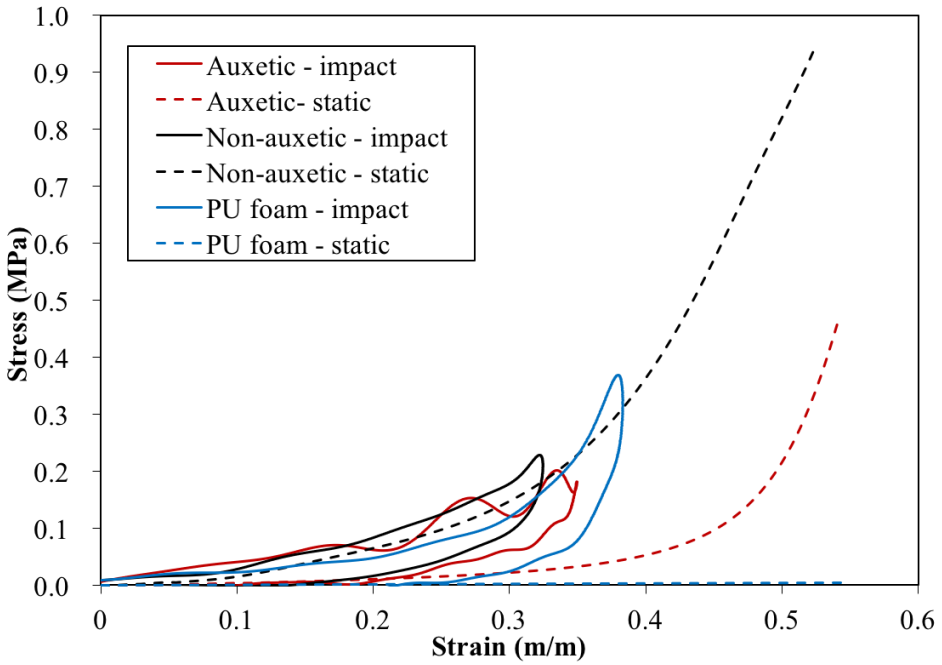

Fig. 12 The stress - strain curves of PU foam, 3D auxetic and non-auxetic textile composites under quasi-static compression and impact tests.

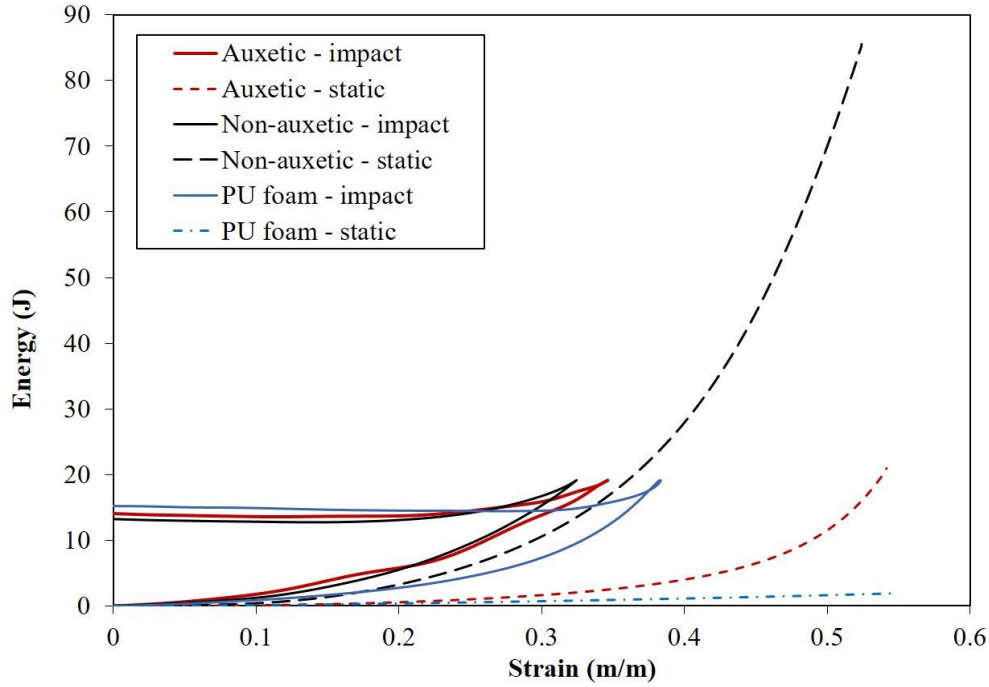

Fig. 13 Energy-strain curves of PU foam, 3D auxetic and non-auxetic textile composites under quasi-static compression and impact tests

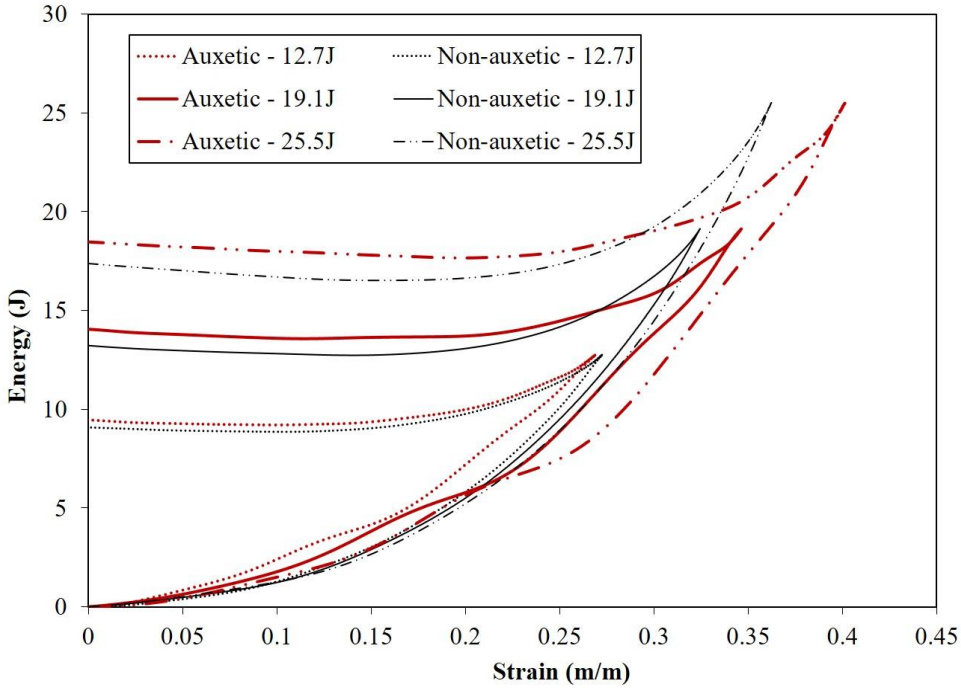

Fig. 14 Energy - strain curve of auxetic and non-auxetic composites under varied impact energies (12.7J, 19.1J and 25.5J).

3.5 Effect of impact energy

Fig. 15 shows the effect of impact energy on the peak contact force and peak transmitted force for both the auxetic and non-auxetic textile composites. It can be seen that both the peak contact force and peak transmitted force increase almost linearly with the increase of the impact energy. This is reasonable because the increase of the initial impact energy can increase the deformation of the composite structure, which results in an increase in peak forces. Under all impact energies, the results show that both the peak contact force and peak transmitted force of the auxetic textile composite are lower than those of the non-auxetic textile composite, which indicate that the auxetic textile composite has better impact protective performance in a range of impact energy. From Fig. 15, it can be also seen that the difference in peak force between the auxetic and non-auxetic textile composites is getting larger with the increase of impact energy as the effect of the maximum negative Poisson's ratio value of the auxetic textile composite also increases with the increase of impact energy. As the increasing speed of the peak contact force and peak transmitted force for the non-auxetic textile composite is higher than that of the auxetic textile composite, the impact protection capacity of the auxetic composite is getting better than that of the non-auxetic composite when the impact energy increases.

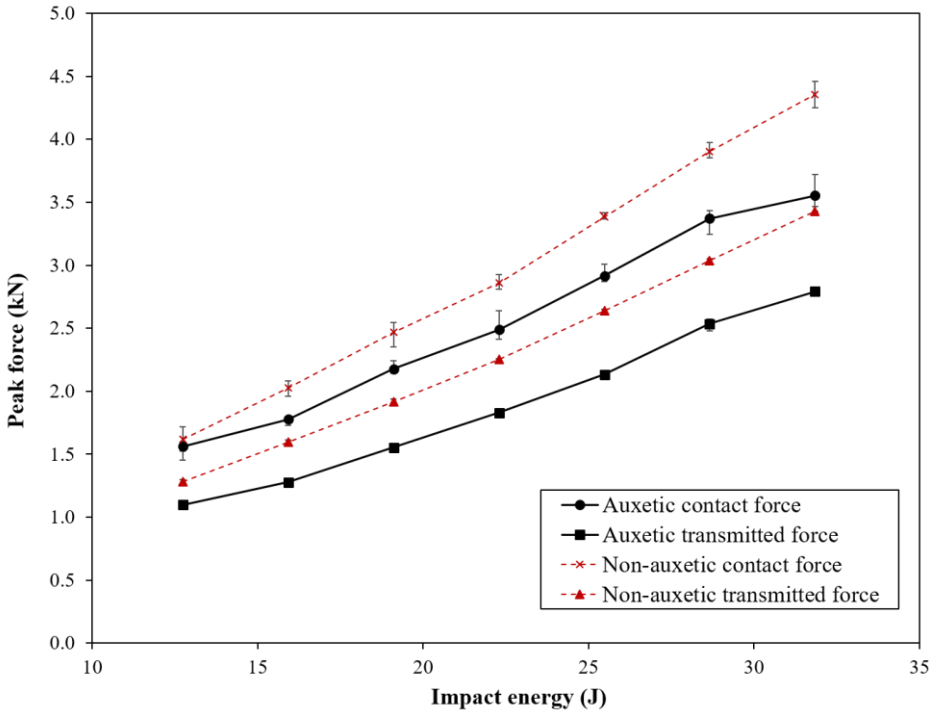

Fig. 15 Effect of impact energy on peak contact force and transmitted force of 3D auxetic and 3D non-auxetic textile composites

3.6 Behaviour under repeating impacts

Fig.16 shows the peak contact force and peak transmitted force of the 3D auxetic and non-auxetic textile composites under repeating impacts at two given impact energy levels (19.1J and 31.9J). It can be seen that the peak contact force fluctuates more than the peak transmitted force, especially at lower impact energy. The results also show that the peak transmitted force tends to be stabilized after the first impact under higher impact energy. As these textile composites are self-fabricated with PU foam as matrix, irregular voids exist in the composite structure. Under each impact, irregular voids may result in different compacting states, causing the variation of the peak contact force. At

higher impact energy level, as the composite structure is easier to be compacted, the difference in compacted state at the end of each impact decreases. Therefore, the variation of the peak contact force decreases. As mentioned before, the warp yarns in the 3D non-auxetic textile structure are arranged in the form of vertical lines. This arrangement results in relatively low stability of the non-auxetic textile composite as the misalignment of the non-auxetic textile structure would happen under each impact, causing the buckling of the composite structure. And the buckling may lead to a non-recovering deformation. Therefore, the 3D auxetic textile composite should have better structural stability than the 3D non-auxetic composite under repeating impacts.

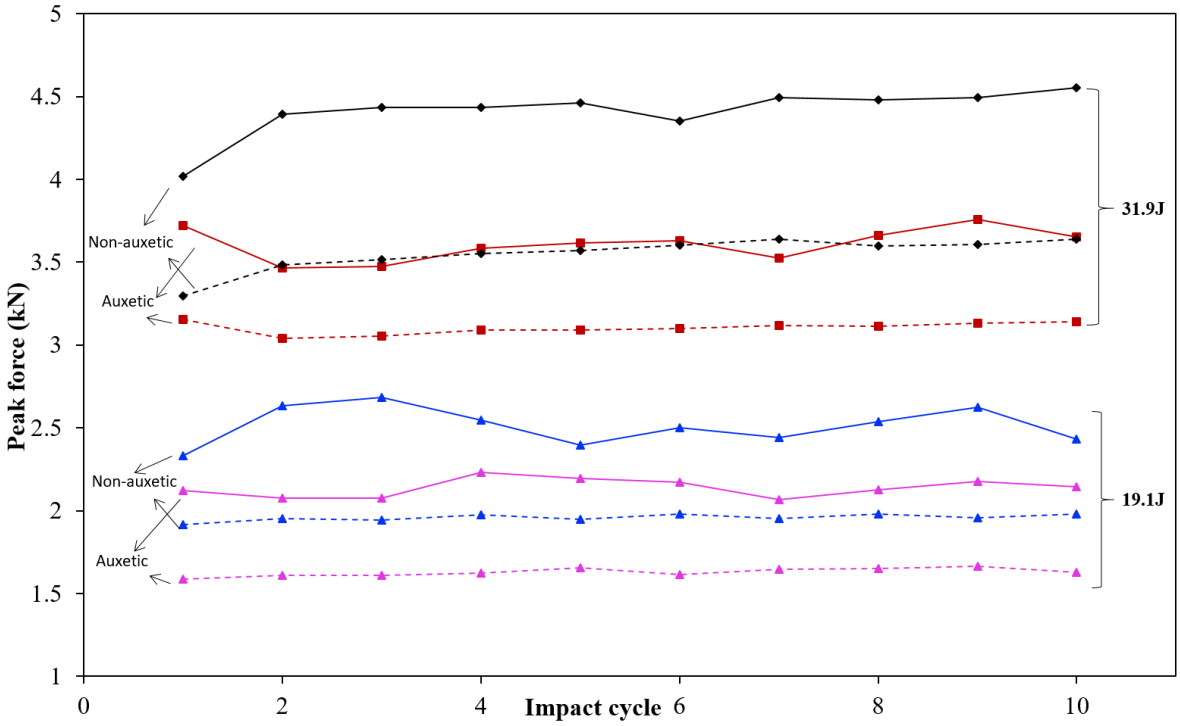

Fig. 16 Peak contact force (solid lines) and peak transmitted force (dash lines) of 3D auxetic and non-auxetic textile composites under repeating impact loading at different impact energy levels (19.1J and 31.9J).

4. Conclusions

Low velocity impact properties of 3D auxetic textile composites were systematically investigated and compared with those of the non-auxetic composites made of the same constituent materials and structural parameters and pure PU foam. Based on the results and analysis, the following conclusions can be drawn.

1) The 3D auxetic textile composite has better impact protective performance than the non-auxetic textile composite due to lower transmitted peak force and higher energy absorption.
2) The mechanical properties of the textile composites under quasi-static compression and impact are different. Under quasi-static compression, the auxetic textile composite behaves much softer and has lower energy absorption than the non-auxetic textile composite. However, under impact test, the difference in mechanical behaviour between the auxetic and non-auxetic textile composites diminishes due to reduction of negative Poisson's ratio effect of the auxetic textile composite. The auxetic composite can absorb more energy than the non-auxetic composite with the increase of impact energy.
3) The auxetic composite has stable impact behaviour under repeating impact testing.

The results of this study demonstrate the potential application of textile composites made of 3D auxetic textile structure as reinforcement for impact protection under low-

velocity impact loading. For the structure design to be optimized and impact performance to be enhanced, further theoretical study is required to better understand their mechanical behaviour under low-velocity impact.

Acknowledgements

The authors would like to thank the funding support from the Research Grants Council of Hong Kong Special Administrative Region Government in the form of a GRF project (No. 515812).

References

1. Alderson, K.L., et al., *How to make auxetic fibre reinforced composites.* Physica Status Solidi B-Basic Solid State Physics, 2005. **242**(3): p. 509-518.
2. Lim, T.C., A. Alderson, and K.L. Alderson, *Experimental studies on the impact properties of auxetic materials.* physica status solidi (b), 2014. **251**(2): p. 307-313.
3. Howell, B., P. Prendergast, and L. Hansen, *Examination of acoustic behavior of negative poisson's ratio materials.* Applied Acoustics, 1994. **43**(2): p. 141-148.
4. Lakes, R.S. and K. Elms, *Indentability of conventional and negative Poisson's ratio foams.* Journal of Composite Materials, 1993. **27**(12): p. 1193-1202.
5. Sanami, M., et al., *Auxetic Materials for Sports Applications.* Procedia Engineering, 2014. **72**: p. 453-458.

6. Evans, K.E. and A. Alderson, *Auxetic materials: Functional materials and structures from lateral thinking!* Advanced Materials, 2000. **12**(9): p. 617-+.

7. Evans, K.E., J.P. Donoghue, and K.L. Alderson, *The design, matching and manufacture of auxetic carbon fibre laminates.* Journal of Composite Materials, 2004. **38**(2): p. 95-106.

8. Herakovich, C.T., *Composite laminate with Nagiave through-thickness Poisson's Ratios.* Journal of Composite Materials, 1984. **18**(5): p. 447-455.

9. Peel, L.D., *Exploration of high and negative Poisson's ratio elastomer-matrix laminates.* Physica Status Solidi B-Basic Solid State Physics, 2007. **244**(3): p. 988-1003.

10. Ge, Z.Y., H. Hu, and Y.P. Liu, *A finite element analysis of a 3D auxetic textile structure for composite reinforcement.* Smart Materials and Structures, 2013. **22**(8): p. 084005.

11. Miller, W., et al., *The manufacture and characterisation of a novel, low modulus, negative Poisson's ratio composite.* Composites Science and Technology, 2009. **69**(5): p. 651-655.

12. Simkins, V.R., et al., *Single fibre pullout tests on auxetic polymeric fibres.* Journal of Materials Science, 2005. **40**(16): p. 4355-4364.

13. Evans, K.E., M.A. Nkansah, and I.J. Hutchinson, *Modeling Negative Poisson Ratio Effects in Network-Embedded Composites.* Acta Metallurgica Et Materialia, 1992. **40**(9): p. 2463-2469.

14. Milton, G.W., *Composite material with Possion's ratio close to -1.* Journal of the Mechanics and Physics of Solids, 1992. **40**(5): p. 1105-1137.

15. Richardson, M. and M. Wisheart, *Review of low-velocity impact properties of composite materials.* Composites Part A: Applied Science and Manufacturing, 1996. **27**(12): p. 1123-1131.

16. Lowe, A. and R. Lakes, *Negative Poisson's ratio foam as seat cushion material.* Cellular Polymers, 2000. **19**(3): p. 157-168.

17. Scarpa, F., L.G. Ciffo, and J.R. Yates, *Dynamic properties of high structural integrity auxetic open cell foam.* Smart Materials & Structures, 2004. **13**(1): p. 49-56.

18. Scarpa, F., et al., *Dynamic crushing of auxetic open-cell polyurethane foam.* Proceedings of the Institution of Mechanical Engineers Part C-Journal of Mechanical Engineering Science, 2002. **216**(12): p. 1153-1156.

19. Lisiecki, J., et al., *Auxetic polyurethane foams-manufacturing and testing*. In book: Proceedings of the Fourth Asian Conference on Mechanics of Functional Materials and Structures, Publisher: Nara Prefectural New Public Hall, 2014. p. 217-220.

20. Allen, T., et al., *Low-kinetic energy impact response of auxetic and conventional open-cell polyurethane foams.* physica status solidi (b), 2015. **252**(7): p. 1631-1639.

21. Rongxing, Z., et al., *An Experimental and Numerical Study on the Impact Energy Absorption Characteristics of the Multiaxial Warp Knitted (MWK)*

Reinforced Composites. Journal of Composite Materials, 2005. **39**(6): p. 525-542.

22. Alderson, K.L. and V.L. Coenen, *The low velocity impact response of auxetic carbon fibre laminates.* physica status solidi (b), 2008. **245**(3): p. 489-496.

23. Liaqat, M., et al., *The development of novel auxetic woven structure for impact applications.* The Journal of The Textile Institute, 2016: p. 1-7.

24. Ge, Z. and H. Hu, *Innovative three-dimensional fabric structure with negative Poisson's ratio for composite reinforcement.* Textile Research Journal, 2012. **83**(5): p. 543-550.

25. Ge, Z., H. Hu, and Y. Liu, *Numerical analysis of deformation behavior of a 3D textile structure with negative Poisson's ratio under compression.* Textile Research Journal, 2014. **85**(5): p. 548-557.

26. Jiang, L.L., B.H. Gu, and H. Hu, *Auxetic composite made with multilayer orthogonal structural reinforcement.* Composite Structures, 2016. **135**: p. 23-29.

27. Jiang, L. and H. Hu, *Low-velocity impact response of multilayer orthogonal structural composite with auxetic effect.* Composite Structures, 2016.

28. Zhou, L., L. Jiang, and H. Hu, *Auxetic composites made of 3D textile structure and polyurethane foam.* physica status solidi (b), 2016: p. 1-11.

29. Zeng, J., H. Hu, and L. Zhou, *A study on negative Poisson's ratio effect of 3D auxetic orthogonal textile composites under compression.* Smart Materials and Structures, 2017. **26**(6): p. 065014.

30. Liu, Y., et al., *Impact compressive behavior of warp-knitted spacer fabrics for protective applications.* Textile Research Journal, 2012. **82**(8): p. 773-788.

31. Jiang, L. and H. Hu, *Finite Element Modeling of Multilayer Orthogonal Auxetic Composites under Low-Velocity Impact.* Materials, 2017. **10**(8): p. 908.